IOPscience iopscience.iop.org

Home Search Collections Journals About Contact us My IOPscience

Modelling of Texture Evolution and Grain Refinement on Complex SPD Paths

This content has been downloaded from IOPscience. Please scroll down to see the full text.

2014 IOP Conf. Ser.: Mater. Sci. Eng. 63 012040

(http://iopscience.iop.org/1757-899X/63/1/012040)

View the table of contents for this issue, or go to the journal homepage for more

Download details:

IP Address: 148.81.55.103
This content was downloaded on 11/08/2014 at 11:08

Please note that terms and conditions apply.

IOP Conf. Series: Materials Science and Engineering **63** (2014) 012040 doi:10.1088/1757-899X/63/1/012040

Modelling of Texture Evolution and Grain Refinement on Complex SPD Paths

K Kowalczyk-Gajewska[1], S Stupkiewicz, K Frydrych and H Petryk

Institute of Fundamental Technological Research (IPPT), Pawinskiego 5b, 02 106 Warsaw, Poland

E-mail: [1]kkowalcz@ippt.pan.pl

Abstract. A computationally efficient procedure for modelling of microstructural changes on complex and spatially nonuniform deformation paths of severe plastic deformation (SPD) is presented. The analysis follows a two-step procedure. In the first step, motivated by saturation of material hardening at large accumulated strains, the steady-state kinematics of the process is generated for a non-hardening viscoplastic model by using the standard finite element method for a specified SPD scheme. In the second step, microstructural changes are investigated along the deformation-gradient trajectories determined in the first step for different initial locations of a material element. The aim of this study is to predict texture evolution and grain refinement in a non-conventional process of cold extrusion assisted by cyclic rotation of the die, called KOBO process, which leads to an ultra-fine grain structure. The texture evolution is calculated for fcc and hcp metals by applying crystal visco-plasticity combined with the self-consistent scale transition scheme. In parallel, by applying the simplified phenomenological model of microstructure evolution along the trajectories, grain refinement is modelled. The results are compared with available experimental data.

1. Introduction

Severe plastic deformation (SPD) processes induce substantial changes in material microstructure such as grain refinement and texture evolution, see the extensive reviews [1, 2, 3, 4] covering different aspects of the problem. To model the microstructure evolution, it is necessary to determine the actual deformation path imposed on the volume element under consideration.

For some well-known SPD processes the macroscopic deformation path is easily determined with a good accuracy by basic kinematics, for instance, for a single pass of ECAP process the simple shear deformation is frequently used [2, 3]. On the other hand, there are processes, such as the KOBO extrusion [5, 6], where the severe plastic deformation field is complex and position-dependent and must be determined numerically, typically by the finite element method. However, a direct use of a material model which requires the history of material parameters to be followed is then difficult due to heavy distortion of finite elements and the need of remeshing. Moreover, a detailed study of texture evolution and grain fragmentation done *simultaneously* with finite element modelling would be extremely time consuming.

That is why a two-step procedure for analysis of microstructure changes in SPD processes has been proposed in [7]. In the first step, the deformation paths for selected material points are determined with the help of the standard finite element method, accompanied by suitable post-


Content from this work may be used under the terms of the Creative Commons Attribution 3.0 licence. Any further distribution of this work must maintain attribution to the author(s) and the title of the work, journal citation and DOI.
Published under licence by IOP Publishing Ltd

processing, by using a non-hardening viscoplastic model. This step, motivated by the observed saturation of material hardening at very large accumulated plastic strains, enables relatively easy calculations of the approximate deformation field for the actual SPD process. A similar approach has been developed in [8] where the velocity gradient components are determined from the analytic flow line functions following from the upper bound method applied to the classical extrusion process. In the approach employed in [7], the deformation gradient paths are determined by directly postprocessing the results of FE simulations of the KOBO extrusion.

In the second step, by applying a refined micromechanical model of plasticity, e.g., the crystal aggregate model or the model of grain refinement, microstructural changes are analyzed along the deformation-gradient trajectories determined in the first step.

In the next sections, principles of the two steps are explained in more detail. Each step is illustrated by examples of the application of the proposed approach to the analysis of microstructure evolution in fcc and hcp materials during the ECAP and the KOBO extrusion processes.

2. Deformation paths in SPD processes

Following the approach proposed in [7], the complex kinematics of SPD processes is determined first by neglecting the material hardening that is saturated at large accumulated plastic strain.

Constitutive equations are specified by the rigid-viscoplastic Norton–Hoff model that relates $\boldsymbol{\sigma}'$, the deviatoric part of the Cauchy stress tensor $\boldsymbol{\sigma}$, and $\mathbf{d}$, the Eulerian strain-rate tensor,

$$\boldsymbol{\sigma}' = \frac{2}{3}\frac{\sigma_{\mathrm{y}}}{d_{\mathrm{II}}^0}\left(\frac{d_{\mathrm{II}}}{d_{\mathrm{II}}^0}\right)^{m-1}\mathbf{d}, \qquad d_{\mathrm{II}} = \sqrt{\frac{2}{3}\,\mathbf{d}\cdot\mathbf{d}}. \tag{1}$$

Here, σ_{y} is the reference yield stress, d_{II}^0 is the reference strain-rate, and $0 < m < 1$ is the strain-rate sensitivity coefficient. In view of incompressibility, we have $\operatorname{tr}\mathbf{d} = 0$.

Since this model behaviour does not depend of the strain history, the finite element method can be used in the Eulerian setting to solve efficiently the boundary value problem for a selected SPD process. The key point is that the procedure simplifies considerably if the kinematics is of steady-state type, so that a single finite element solution is only needed to determine by appropriate post-processing the whole deformation path for any material point.

The procedure can be applied to different SPD processes. In this paper, the extrusion assisted by cyclic rotation of the die (the KOBO process) is taken as the basic example and compared with the commonly known ECAP process.

The principle of the KOBO extrusion process [5, 6] is illustrated in figure 1. It is a non-conventional process of cold extrusion where the hollow die is not fixed but subjected to cyclic rotation (figure 1a). In result, the plastic flow pattern differs from the usual extrusion scheme and takes the form shown in figure 1b [7]. As explained in the reference, under the assumption of non-hardening, the quasi-static solution of the problem of axisymmetric extrusion with cyclic torsion can be easily constructed from the solution for steady-state extrusion with monotonic torsion. This is done by changing the sign of the angular velocity in a cyclic manner while the radial and axial velocities remain the same as in the steady-state solution.

The deformation gradient along material point trajectories shown in figure 1b varies in a manner strongly dependent on the initial position of the point. This is shown in figure 2 by assuming for illustrational purposes a spherical shape of a material element at some selected stage of the deformation (the whole deformation path would correspond to the element elongation too large to be visualized). Figure 2 shows how an assumed sphere deforms and rotates along the subsequent segment of the deformation path.

For the sake of comparison, examples of deformation histories for the known different variants of the ECAP process are shown in figure 3.

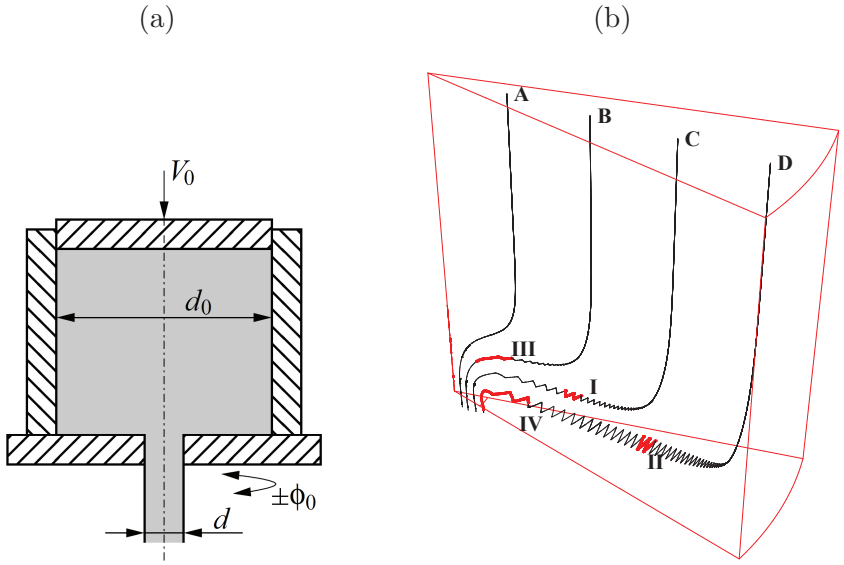

Figure 1. (a) Geometry of the KOBO extrusion process and (b) trajectories of four material points determined by finite element calculations for a non-hardening material obeying Eq. (1) and for process parameters: $\phi_0 = \pm 8^o$, $d_o : d = 40 : 4$ [mm], $f = 5$ [Hz], $V_0 = 0.5$ [mm/s]. Segments of the deformation paths analyzed in figure 2 are marked in red.

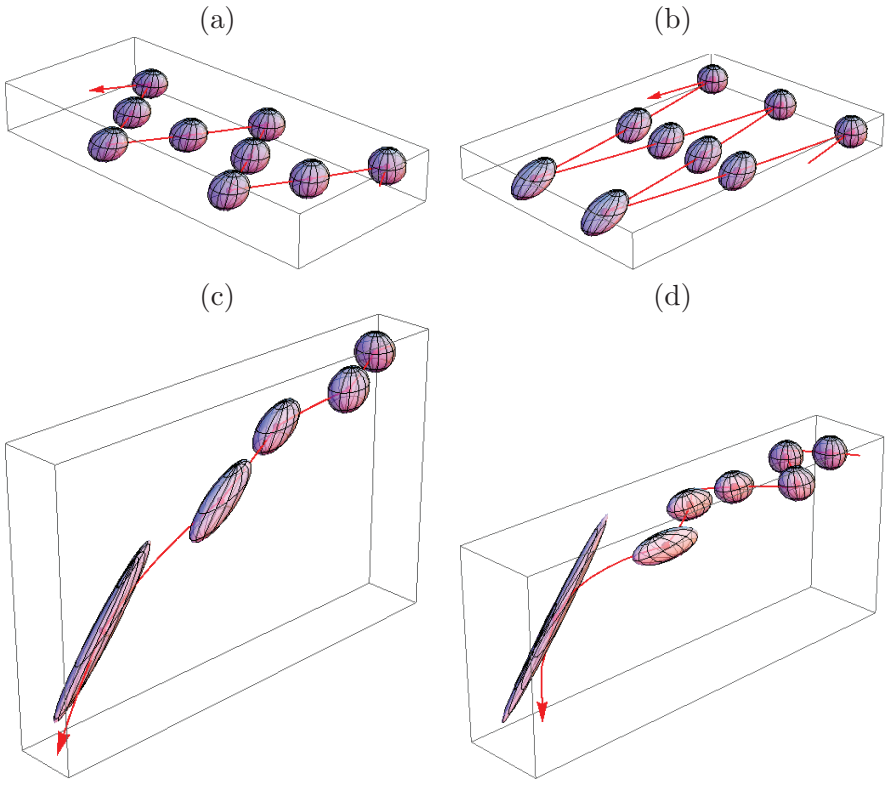

Figure 2. Deformation of a volume element in the KOBO extrusion process on the segments of the deformation paths marked in red in figure 1b: (a) I, (b) II, (c) III, (d) IV;

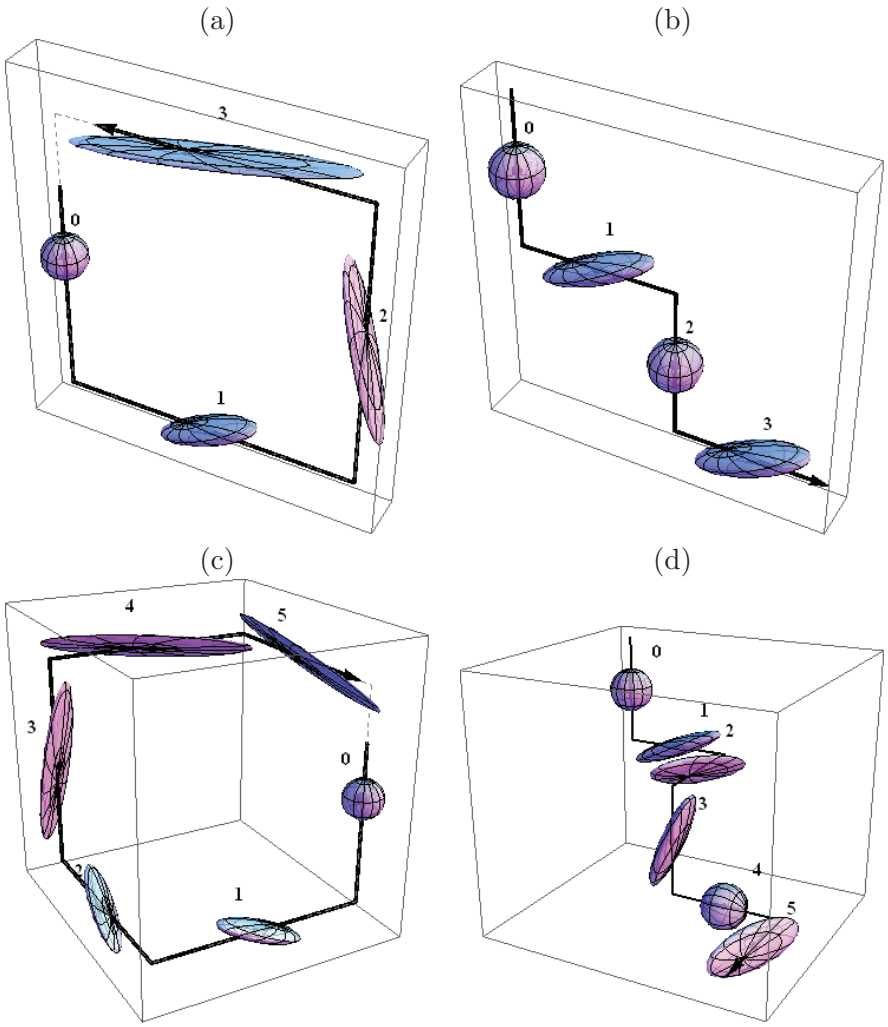

Figure 3. Deformation of a volume element in multiple pass ECAP process (a) Route A, (b) Route C (b), Route Ba (c), Route Bc (d);

Some similarities are found between those deformation schemes and the ones on subsequent segments of the deformation path in the KOBO extrusion. Reversible simple shear deformation of volume elements is observed in the regimes of cyclic shearing (e.g., segments I and II), corresponding to the route C in the ECAP process, so that after a single cycle of die rotation the initial shape is approximately recovered. The shear amplitude is, in general, smaller than in the ECAP process. It depends on the process parameter ϕ_0 and decreases for the deformation paths closer to the axis of extruded rod. On the other hand, as multiple cycles are performed on the volume element in the KOBO extrusion, accumulated plastic strain is usually much larger than in the ECAP process. Close to the zone of material outflow from the die (e.g., segments III and IV) the deformation scheme changes towards the one observed in Route A and Route Ba of the ECAP process, for which distortion of the volume element accumulates as deformation proceeds. Observe, however, that, in the KOBO extrusion, distortion connected with the accumulated simple shear is additionally enhanced by isochoric elongation of ellipsoids characteristic for the classical extrusion process. This type of deformation dominates in the central part of extruded sample.

Heterogeneity of deformation in the KOBO process results in a non-uniform grain refinement and a non-uniform texture after the process, as will be shown below.

3. Modelling of microstructure evolution

3.1. Grain refinement

A quantitative model of grain refinement developed in [9] is briefly outlined below. The model describes, in a phenomenological manner, the experimentally observed microstructural effects that accompany severe plastic deformation processes in metals. The relevant references to experimental literature can be found in [9]; see also the interesting approach, formulated within the crystal plasticity framework, proposed more recently in [10].

In order to account for transitory periods of transformation and reconstruction of dislocation microstructure after strain-rate reversals, during which dislocation multiplication and work-hardening are slowed down, the *effective plastic strain* $\varepsilon_{\mathrm{eff}}$ is introduced that is related to the equivalent (von Mises) strain $\varepsilon_{\mathrm{vM}}$ by the following evolution equation

$$\dot{\varepsilon}_{\mathrm{eff}} = \begin{cases} \dot{\varepsilon}_{\mathrm{vM}} & \text{if } \mathbf{d}^{\mathrm{p}} \cdot \mathbf{e}_{\mathrm{r}} > 0 \text{ and } \|\mathbf{e}_{\mathrm{r}}\| > r, \\ 0 & \text{otherwise,} \end{cases} \tag{2}$$

where $\mathbf{e}_{\mathrm{r}}$ is the back-strain tensor defined below, $\mathbf{d}^{\mathrm{p}}$ is the plastic part of the Eulerian strain rate, $\dot{\varepsilon}_{\mathrm{vM}} = (\frac{2}{3}\mathbf{d}^{\mathrm{p}} \cdot \mathbf{d}^{\mathrm{p}})^{1/2}$, $r = r^{\infty}(1 - e^{-\varepsilon_{\mathrm{eff}}/\varepsilon_{\mathrm{r}}})$, and r^{∞} and ε_{r} are material constants. The back-strain (prestrain) tensor $\mathbf{e}_{\mathrm{r}}$ is defined incrementally as follows

$$\overset{\nabla}{\mathbf{e}}_{\mathrm{r}} = \mathbf{d}_{\mathrm{p}} - \mathbf{e}_{\mathrm{r}}\|\mathbf{d}_{\mathrm{p}}\|/\varepsilon_{\mathrm{r}} \tag{3}$$

where $\overset{\nabla}{\mathbf{e}}_{\mathrm{r}}$ denotes the objective corotational (Zaremba–Jaumann) rate of $\mathbf{e}_{\mathrm{r}}$.

Several parameters are then introduced that describe the microstructure formed in a metal during large plastic deformation. Following numerous experimental observations, the microstructure is assumed to be composed of equiaxed ordinary dislocation cells and cell-block domains. The microstructure is described by parameters D_{c}, D_{b} and D_{w} denoting, respectively, the mean dislocation-cell diameter, the mean domain-wall spacing and the mean cell-block length, and simple evolution laws are postulated for those parameters. Using those parameters, the fraction of high-angle grain boundaries (HAGB), denoted by ξ_{h}, can be estimated according to

$$\xi_{\mathrm{h}} = \frac{D_{\mathrm{c}}}{3}\left(\frac{1}{D_{\mathrm{b}}} + \frac{1}{D_{\mathrm{w}}}\right). \tag{4}$$

Evolution of the microstructure parameters D_{c}, D_{b} and D_{w} is expressed in terms of the effective plastic strain $\varepsilon_{\mathrm{eff}}$ defined above. In contrast to the von Mises strain $\varepsilon_{\mathrm{vM}}$, the effective plastic strain $\varepsilon_{\mathrm{eff}}$ does not increase during transitory periods after strain-rate reversals. Hence, according to the model (and in agreement with experimental evidence), grain refinement is slowed down during cyclic deformation as compared to the monotonic deformation characterized by the same accumulated von Mises strain $\varepsilon_{\mathrm{vM}}$.

The microstructure parameters can be used to estimate strain hardening during large plastic deformation. Specifically, the following formula for the isotropic part of the yield stress σ_{y} has been postulated,

$$\sigma_{\mathrm{y}} = \sigma_1 + (1 - \xi_{\mathrm{h}})k_{\mathrm{c}}Gb\frac{1}{D_{\mathrm{c}}} + \xi_{\mathrm{h}}k_{\mathrm{b}}\frac{1}{\sqrt{D_{\mathrm{b}}}}, \tag{5}$$

where σ_1 is interpreted as a frictional stress, G denotes the elastic shear modulus, b is the magnitude of the Burgers vector, and coefficients k_{c} and k_{b} are material constants. Equation (5) combines the well-known formulae for dislocation strengthening, inversely proportional to

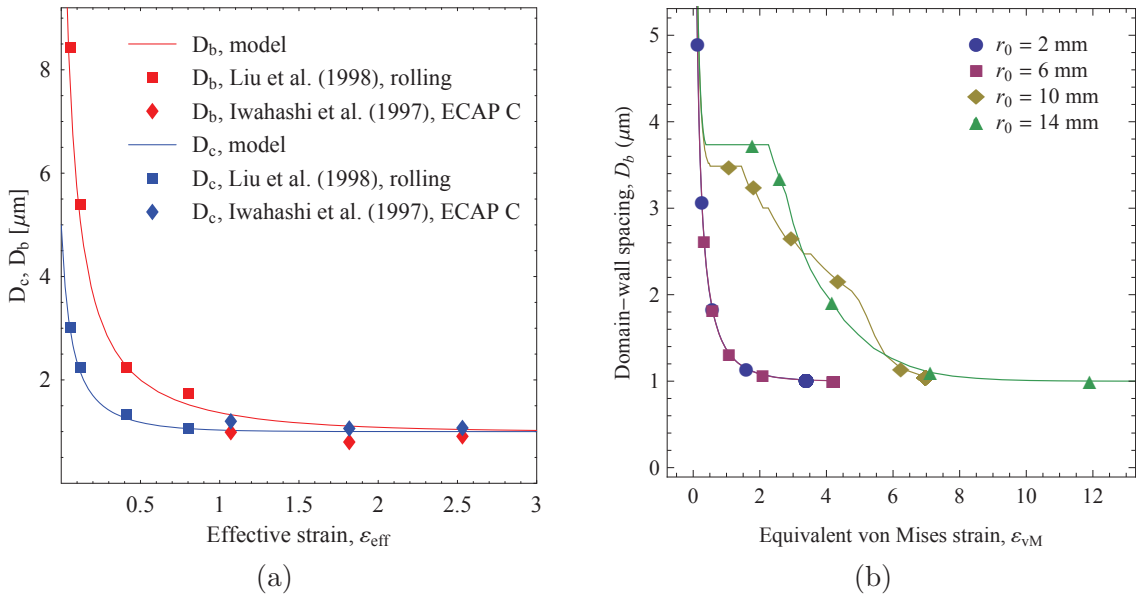

Figure 4. Sample predictions of the grain refinement model [9] for pure aluminum: (a) mean dislocation-cell diameter D_c and mean domain-wall spacing D_b as a function of the effective plastic strain ε_{eff} [9], (b) evolution of the mean domain-wall spacing D_b along selected trajectories during KOBO extrusion [7].

dislocation cell size D_c, and high-angle boundary strengthening, expressed by a relationship of the Hall–Petch type involving the high-angle boundary spacing D_b. The two contributions are weighted using the low- and high-angle boundary area fractions $1 - \xi_h$ and ξ_h, respectively.

Predictions of the model are illustrated in figure 4. Figure 4a shows the evolution of microstructure parameters D_c and D_b predicted for pure aluminium processed by rolling and ECAP (route C), cf. [9]. The parameters are shown as a function of the effective plastic strain ε_{eff} defined by Eq. (2) so that the two processes are characterized by the same curve, despite the strain paths are different. It is seen that the predictions match experimental data [11, 12] very well. Figure 4b shows evolution the mean domain-wall spacing D_b in pure aluminium processed by KOBO extrusion, cf. [7]. Here, selected trajectories of different initial radius r_0 are parametrized by the von Mises strain ε_{vM}. The effect of strain path on the evolution of microstructure is clearly visible.

3.2. Texture development

Simulations of texture evolution in a fcc material subjected to the KOBO extrusion process have been reported in [13]. Selected results are invoked in figure 5. It has been assumed that material deforms only by the basic slip systems $\{111\}\langle 110\rangle$. It has been found that the texture development, due to differences in the deformation paths discussed above, is strongly heterogeneous depending on the location of the volume element. For the center of the extruded rod, the texture evolves similarly to the conventional extrusion process, while strong textures develop in the outer parts of the rod. In the open literature, the experimental data concerning the texture development in the KOBO extrusion process are far more scarcer than for the ECAP process. As concerns fcc materials, in a conference communication [14] it is reported that single blocks of orientations are observed in the regions subjected to the intensive cyclic shearing deformation, and the typical fiber texture is formed in the center of the extruded rod, which qualitatively agrees with the modelling predictions.

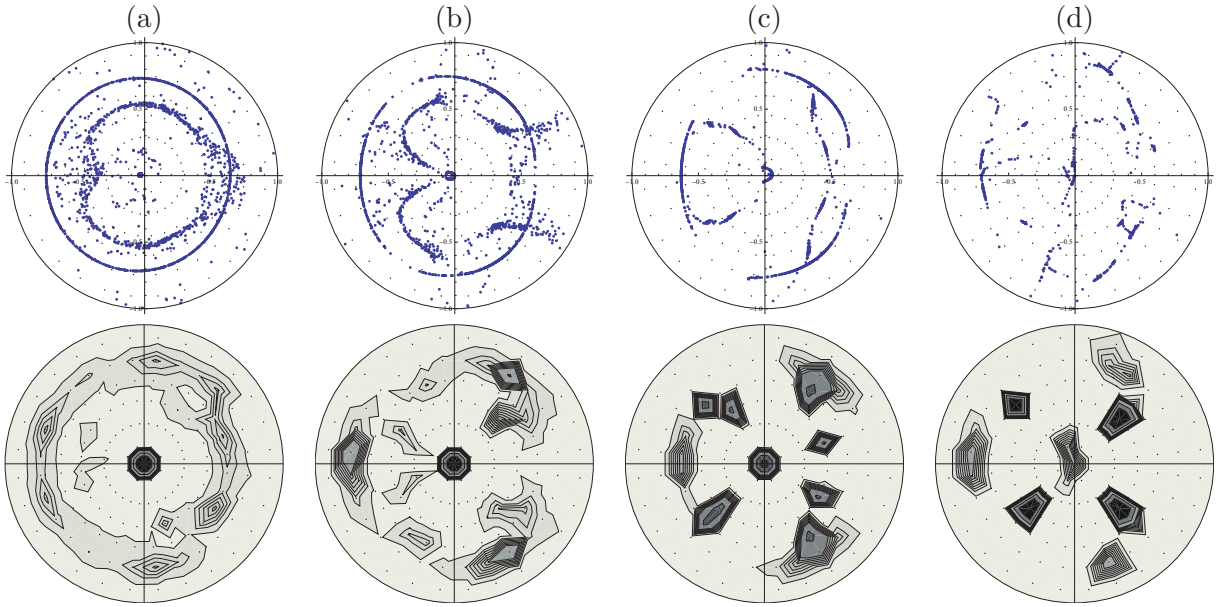

Figure 5. Texture evolution in fcc material for the KOBO extrusion with the process parameters: $\phi_0 = \pm 4^o$, $d_o : d = 40 : 8$ [mm], $f = 4$ [Hz], $V_0 = 1$ [mm/s], pole figure {111}, for: a) $r = 0$ [mm], b) $r = 1.2$ [mm], c) $r = 2.4$ [mm], d) $r = 3.6$ [mm] ($r : r_0 = 0.2$); aggregate of 500 orientations [13]

In this contribution, we present new results of texture simulation for an hcp material: AZ31B magnesium alloy, which is a material of high specific strength that deforms by slip and twinning. Twinning is activated due to insufficient number of easy slip systems in this alloy. Note that the KOBO extrusion process proved to be an efficient forming process for the materials of low ductility [6] for which traditional methods often fail to deliver acceptable products.

The texture evolution model used in this work combines the large strain crystal plasticity model accounting for twinning with the self-consistent grain-to-polycrystal scale transition scheme. General outline of the theory can be found in [15, 16], while the details of incorporation of twinning – in [17]. Basic features of the model are described below.

Multiplicative decomposition of the deformation gradient of a single grain into the elastic and plastic parts is applied. It is assumed that the elastic stretches are negligible compared to the plastic strains so that the elastic part is restricted to a rigid rotation responsible for the texture development. Plastic deformation occurs by slip or twinning on the slip or twin systems relevant for the considered material.

Twinning is described as a uni-directional slip mode. Appearance of twin related orientations in the texture image is accounted for using the statistical concept of Van Houtte [18] modified in [17] in order to preserve consistency of twinning activity, and the resulting twin volume fraction in the grain, with the reorientation probability. It is achieved using the probabilistic twin volume consistent scheme (PTVC) proposed in [17].

The rate of slip or pseudo-slip on the considered slip or twin system r is related to the resolved shear stress τ^r according to the viscoplastic power law

$$\dot{\gamma}^r = \dot{\gamma}_0 \, \mathrm{sign}(\tau^r) \left| \frac{\tau^r}{\tau_c^r} \right|^n . \tag{6}$$

The critical shear stress τ_c^r evolves according to the hardening law proposed in [17]. This law includes four types of interactions: slip-slip, slip-twin, twin-slip and twin-twin and differentiates

between their impact on the increment of τ_c^r. In short, the formula describing the current hardening modulus due to slip-slip or twin-slip interaction is the Voce-type law with saturation [19] accounting for the athermal statistical storage of moving dislocations and dynamic recovery, while a current hardening modulus due to slip-twin or twin-twin interaction is proportional to $f^{TW}/(1-f^{TW})$, where f^{TW} is the current twin volume fraction. It describes the geometrical effect of twin boundaries on deformation modes activity [20]. More details concerning the formulation can be found in [17, 21].

The response of a polycrystalline aggregate is obtained by averaging the responses of individual grains in the representative volume element (RVE). The most common Taylor model, assuming the same deformation in each grain, usually does not provide acceptable results in the case of materials and complex processes under consideration. Metals deforming by slip and twinning often have less than five independent slip systems, which leads to an overestimation of the overall stress when using the Taylor model. The self-consistent schemes making use of the Eshelby solution provide better estimates. Note that for non-linear material behaviour different variants of the self-consistent approach are available. They are not discussed here in more detail. The reader is referred to the related publications, e.g. [22, 21]. Computations reported in this paper were performed using the VPSC code [16], in the frame of which own procedures for the PTVC reorientation scheme and the developed hardening model have been implemented.

In calculations, four deformations modes are assumed to be potentially active for the AZ31B magnesium alloy: basal $(0001)\langle 11\bar{2}0\rangle$, prismatic $\{1100\}\langle 11\bar{2}0\rangle$ and pyramidal $\langle c+a\rangle$ $\{1122\}\langle 11\bar{2}3\rangle$ slip systems as well as tensile twinning $\{10\bar{1}2\}\langle 10\bar{1}1\rangle$. Material parameters used in the crystal plasticity model can be found in [21]. Aggregates of 500 grains, initially without texture, are analyzed. They are subjected to the deformation paths obtained using the procedure described in Section 2 for the KOBO extrusion with the process parameters specified in the figure captions. They are the same as those applied in [23] where textures after KOBO extrusion have been studied experimentally along the axial cross-section of the rod for the material under consideration.

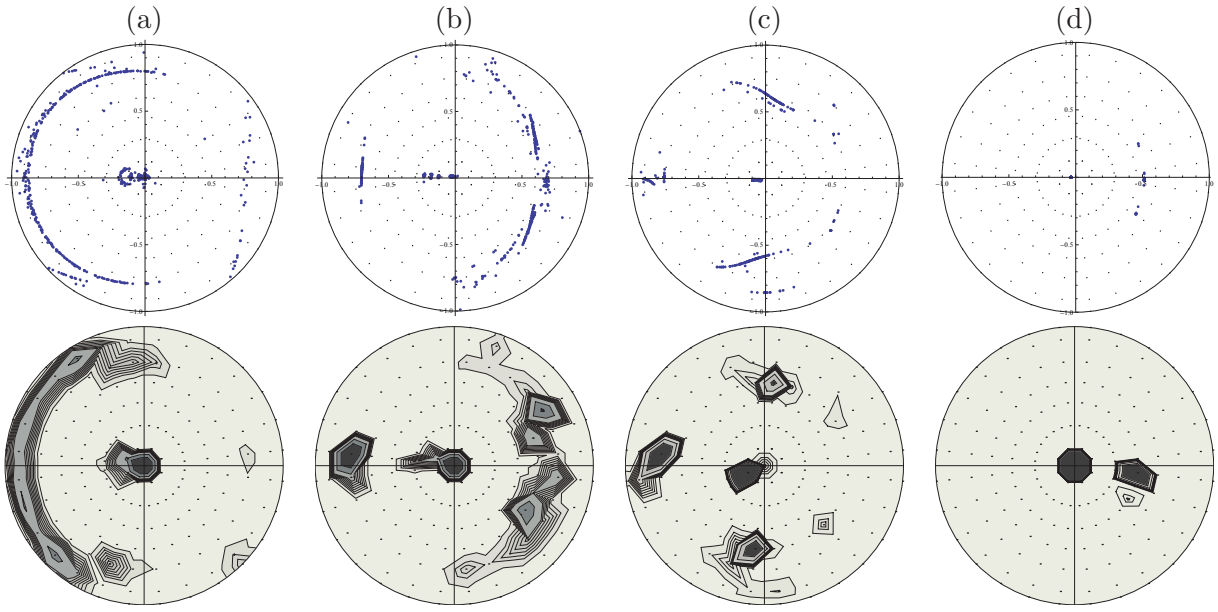

Figure 6. Texture evolution in AZ31B Mg alloy for the KOBO extrusion with the process parameters: $\phi_0 = \pm 8^o$, $d_o : d = 40 : 4$ [mm], $f = 5$ [Hz], $V_0 = 0.5$ [mm/s], pole figure (0001) for: a) $r = 0.45$ [mm], b) $r = 0.9$ [mm], c) $r = 1.35$ [mm], d) $r = 1.8$ [mm] $(r : r_0 = 0.1)$; aggregate of 500 orientations

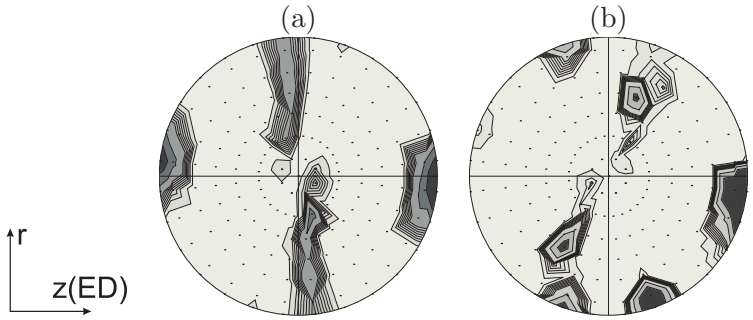

Figure 7. Texture evolution in AZ31B Mg alloy for the KOBO extrusion with the process parameters: $\phi_0 = \pm 8^o$, $d_o : d = 40 : 4$ [mm], $f = 5$ [Hz], $V_0 = 0.5$ [mm/s], pole figure (0001) projected on r-z plane for a) $r = 0.45$ [mm] and b) $r = 0.9$ [mm] ($r : r_0 = 0.1$); aggregate of 500 orientations

The (0001) pole figures obtained for the AZ31B polycrystal (figure 6) show final texture for the assumed initial location of the material volume element. Similarly to the fcc material (figure 5), the results are presented in two ways: discrete point plots containing the orientation of each pole for each of 500 grains and contour plots showing the reconstructed orientation distribution functions for the same set of data. The extrusion axis is perpendicular to the projection plane and the radial direction is aligned with the horizontal axis of the figure. Qualitatively, the results are similar to those obtained for the fcc material, i.e., due to differences in the deformation paths, the texture varies strongly depending on the location of the volume element. Again, for the center of the rod the texture corresponds to the one obtained for the conventional extrusion process (not shown here), while outside of the cylinder axis the texture image loses axial symmetry and only the symmetry with respect to the horizontal axis is visible. The strong texture, characterized by single orientation blocks, are found for the elements located close to the lateral boundary of the rod (see figures 6c,d).

Figure 7 presents the contour plots of (0001) pole figures. Here, the extrusion axis is coaxial with the projection plane, and the radial direction is aligned with the vertical axis of the pole figure. The texture visualizations in figure 7 bear some resemblance to the experimental data reported in [23], especially concerning the main texture component, although a direct comparison is not possible due to the lack of detailed information concerning the location and dimensions of measurement sites.

To the authors' best knowledge a systematic experimental study of texture heterogeneity along the cross-sections of the KOBO extruded rode is still lacking. The presented modelling results may serve as a good starting point for planning relevant testing strategy for such a study.

4. Conclusions

It has been demonstrated that the proposed two-step procedure for the modelling of microstructural changes on complex and spatially nonuniform deformation paths of severe plastic deformation is computationally effective. The essence of the first step is to determine deformation-gradient trajectories for selected elements in the material sample by using the finite element method, neglecting a possible hardening effect on the deformation field. This approximation is needed since otherwise the problem is difficult to handle numerically. Different deformation paths have been illustrated graphically in figures 2 and 3 for KOBO and ECAP processes. In the second step, the deformation paths determined in the first step have been used to investigate microstructural changes such as grain refinement and texture evolution. A qualitative comparison to the available experimental data looks promising. However, a

definite conclusion about the predictive capabilities of the proposed procedure regarding the real behaviour of materials subjected to complex SPD requires yet further work.

Acknowledgements
The research were partially supported by the project of the National Science Center (NCN) granted by the decision No. DEC-2013/09/B/ST8/03320

References

[1] Valiev R Z, Islamgaliev K, and Alexandrov I V 2000 Bulk nanostructured materials from severe plastic deformation *Progress Mater. Sci.* **45** 103–89
[2] Valiev R Z and Langdon T G 2006 Principles of equal-channel angular pressing as a processing tool for grain refinement *Progress Mater. Sci.* **51** 881–981
[3] Beyerlein I J and Toth L S 2009 Texture evolution in equal-channel angular extrusion *Progress Mater. Sci.* **54** 427–510
[4] Langdon T G 2013 Twenty-five years of ultrafine-grained materials: Achieving exceptional properties through grain refinement *Acta Mater.* **61** 7035–59
[5] Korbel A and Bochniak A 1995 The structure based design of metal forming operations *J. Mat. Proc. Technol.* **53** 229–37
[6] Bochniak W and Korbel A 2000 Plastic flow of aluminium extruded under complex conditions *Mater. Sci. Techn.* **16** 664–69
[7] Petryk H and Stupkiewicz S 2012 Modelling of microstructure evolution on complex paths of large plastic deformation *Int. J. Mat. Res.* **103** 271–77
[8] Gu C F, Toth L S, Lapovok R, Davies C H J 2011 Texture evolution and grain refinement of ultrafine-grained copper during micro-extrusion *Philos. Mag.* **91** 273–290
[9] Petryk H and Stupkiewicz S 2007 A quantitative model of grain refinement and strain hardening during severe plastic deformation *Mater. Sci. Eng. A* **444** 214–19
[10] Toth L S, Estrin Y, Lapovok R, Gu C F 2010 A model of grain fragmentation based on lattice curvature *Acta Mater.* **58** 1782–1794
[11] Iwahashi Y, Horita Z, Nemoto M, and Langdon T G 1997 An investigation of microstructural evolution during equal-channel angular pressing *Acta Mater.* **45**(11) 4733–41
[12] Liu Q, Juul Jensen D, and Hansen N 1998 Effect of grain orientation on deformation structure in cold-rolled polycrystalline aluminium *Acta Mater.* **46**(16) 5819–38
[13] Kowalczyk-Gajewska K and Stupkiewicz S 2013 Modelling of texture evolution in kobo extrusion process *Arch. Metal. Mater.* **58** 113–18
[14] Korbel A, Błaż L, Stalony-Dobrzański F, Bonarski J, Tarkowski L, and Pospiech J 2008 Characterization methods for metallic materials deformed in the large strain regime (in Polish) Presented at PlastMet VI Seminar, Łańcut
[15] Asaro R J 1983 Micromechanics of crystals and polycrystals *Adv. Appl. Mech.* **23** 1–115
[16] Lebensohn R A and Tomé C N 1993 A self-consistent anisotropic approach for the simulation of plastic deformation and texture development of polycrystals: Application to zirconium alloys *Acta Metall. Mater.* **41** 2611–24
[17] Kowalczyk-Gajewska K 2010 Modelling of texture evolution in metals accounting for lattice reorientation due to twinning *Eur. J. Mech. Solids/A* **29** 28–41
[18] Van Houtte P 1978 Simulation of the rolling texture and shear texture of brass by the Taylor theory adapted for mechanical twinning *Acta Metal.* **26** 591–604
[19] Kalidindi S R, Bronkhorst C A, and Anand L 1992 Crystallographic texture evolution in bulk deformation processing of fcc metals *J. Mech. Phys. Solids* **40** 537–69
[20] Karaman I, Sehitoglu H, Beaudoin A J, Chumlyakov Y I, Maier H J, and Tomé C N. 2000 Modeling the deformation behavior of Hadfield steel single and polycrystals due to twinning and slip *Acta Mater.* **48** 2031–47
[21] Kowalczyk-Gajewska K 2011 *Micromechanical modelling of metals and alloys of high specific strength* (IFTR Reports 1/2011 Warsaw)
[22] Molinari A, Ahzi S, and Kouddane R 1997 On the self-consistent modeling of elastic-plastic behavior of polycrystals *Mech. Mater.* **26** 43–62
[23] Pospiech J, Korbel A, Bonarski J, Bochniak W, and Tarkowski L 2008 Microstructure and texture of Mg-based AZ alloys after heavy deformation under cyclic strain path change conditions *Mater. Sci. Forum* **584–586** 565–70